ICAS 2016
30th Congress of the International Council of the Aeronautical Sciences
DCC, Daejeon, Korea | September 25-30, 2016

NOVEL PILOT CONTROL MODEL WITH STOCHASTIC AND PERIODICAL MOVEMENT

Ryota Mori*
***Electronic Navigation Research Institute**

Keywords: *pilot model, landing, human factor*

Abstract

A new pilot column control model is proposed. The conventional model applied in other researches is based on a transfer function, which cannot model stochastic and periodical movement observed in actual pilot control data. This paper focuses on the lateral control (roll control), and investigates the effectiveness of the proposed model. First, the actual pilot control data is obtained under different wind conditions. The parameters in the proposed pilot model are optimized based on the actual pilot control data. The obtained pilot models are verified through landing simulations. The simulation results show that the proposed model captures the pilot control characteristics very well.

1 Introduction

Aircraft landings have become safer and more reliable due to the introduction of the Instrument Landing System (ILS). ILS provides both lateral and vertical guidance, and enables landing under bad visibility conditions. Although ILS guidance is very accurate, the aircraft can still deviate from the nominal path due to its navigation error, wind effects, etc. Therefore, to avoid collision from the ground obstacles, a protection area is set around the ILS nominal path according to ICAO PANS-OPS[1]. Consequently, ILS cannot be installed at some airports or runways where the protection area is in the way. These rules were developed in 1970s and have not been updated. Recently, a new GPS-based landing system (called GLS: GBAS Landing System) has gained popularity as it can provide more accurate guidance than ILS. If this accuracy improvement is taken into consideration, the required protection area will shrink. Moreover, the aircraft performance itself has also been improved since the criteria were developed. The protection area size is affected by both navigation performance and aircraft performance. Therefore, the protection area can be further reduced by considering the aircraft performance as well as the navigation performance.

To evaluate the protection area, simulation-based approach is straightforward. However, the simulation environment requires several components, such as the navigation error model, wind model, the aircraft dynamics model. ILS/GLS approach is usually operated by pilot manual control, so a pilot control model is also required. To avoid the underestimation of the collision risk, various pilot control characteristics should be implemented to model the aircraft path tracking error precisely. This research focuses on the development of a pilot manual control model suitable for the evaluation of the protection area. Since the previous research focused on the longitudinal motion[2], this paper considers the lateral motion, i.e. aileron control.

2 Characteristics of Pilot Control and the Proposed Pilot Model

2.1 Target of This Study

The target phase of the study is the final descent phase, because the protection area is set around the final descent path. The final descent means that the aircraft captures both glideslope and localizer, and flies straight maintaining a fixed descent angle following the glideslope and localizer guidance. During this phase, the pilot mainly tracks the flight director (FD) guidance

provided by automatic flight directory system (AFDS). Figure 1 shows the image of the primary flight display (PFD), which the pilot mainly watches during the final descent phase. There are two magenta horizontal and vertical bars, which indicate the desired pitch and roll angles (i.e. pitch and roll commands). When the current pitch angle and roll angles are the same as the pitch command and roll command, FD bars cross at the center.

Fig. 2 shows the pilot control flow based on FD commands. First, FD command generator creates FD pitch/roll commands. The difference of FD pitch/roll commands and actual pitch/roll angles is shown as PFD bars on PFD. Second, the pilot controls control stick based on FD bars information. Third, the aircraft moves based on its dynamics, pilot control, and wind disturbances. This loop is repeated continuously. In this flow, the pilot control is simple, just track the FD commands. FD command generator is developed based on PID control theory, and the parameters are tuned so that the pilot can control the aircraft without problems based on FD command. The development of FD command is out of scope of this research, so these details will be omitted.

Fig. 1 Primary Flight Display.

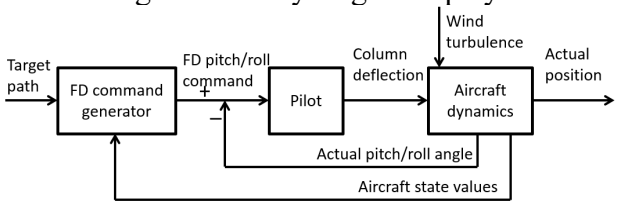

Fig. 2 Pilot control flow.

2.2 Data acquisition

First, flight data is obtained to analyze and model the pilot control. This time, the flight data is obtained via flight simulator. The aircraft model is Dornier 228-202, which is a small turbo-prop aircraft. The aircraft used here is an experimental aircraft owned by Japan Aerospace Exploration Agency (JAXA). This flight simulator can create counter force and realistic data can be obtained. One pilot has collaborated in this experiment. He is a retired captain pilot with experience of B747-400. New-Chitose Airport (RJCC) Runway 01L is assumed in the simulation, and three wind patterns are used as summarized in Table 1. The turbulence is created by a Von Karman model[3]. The pilot controls the aircraft five times: three times for wind (i), and once for wind (ii) and wind (iii). Each data set is described like "data (i)-1". The aircraft starts flying before capturing the localizer and the glideslope, and captures the localizer prior to capturing the glideslope. The final descent starts at an altitude of 2000 ft. The autothrottole is activated, so no manual thrust control is required. The autothrottle is developed based on PID control theory.

Table 1 Wind parameters.

Wind	Steady wind	Turbulence
(i)	10 kt from 45 deg direction	Light
(ii)		Moderate
(iii)	None	None

2.3 Characteristics of Pilot Control in Longitudinal Motion

Since the longitudinal control model was proposed in the previous research, this paper considers the lateral motion. The question is whether the same model can be applied to the lateral control model as well. First, the control characteristics between longitudinal and lateral control are compared. Fig. 3 shows the time histories of lateral control and motion, and Fig. 4 shows the time histories of longitudinal control and motion. The observed characteristics in pitch control are the following: 1) stochastic behavior, 2) periodic behavior, 3) discrete behavior, and 4) half control. These four behaviors are explained in detail.

1) Stochastic behavior

Since the human pilot is not an automatic controller, the human pilot control varies even under the same conditions. Overshoot is also observed.

2) Periodic behavior

About 2 s periodical control is observed in both pitch angle and control movement. According to the data analysis, the pitch command does not include this 2 s oscillation component. The periodic movement seems a pilot's self-oscillation.

3) Discrete behavior

A human pilot usually conducts a discrete movement, not a continuous movement, while an automatic controller (such as autopilot) conducts a continuous movement.

4) Half control

Half control is a pilot's control strategy, where the pilot moves the control stick only half of what is required to avoid over-control. On the other hand, this half control seems to cause command tracking delay.

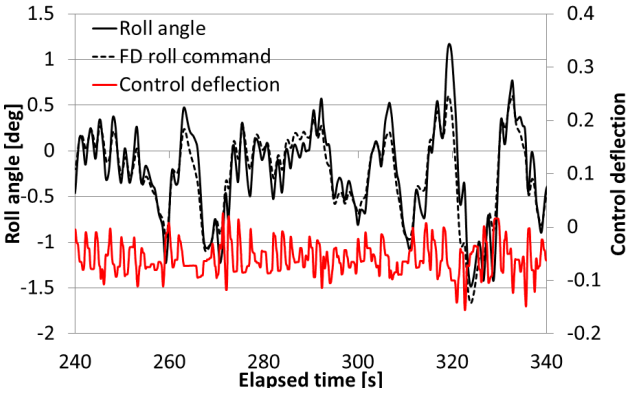

Fig. 3 Lateral control and movement of data (i)-1.

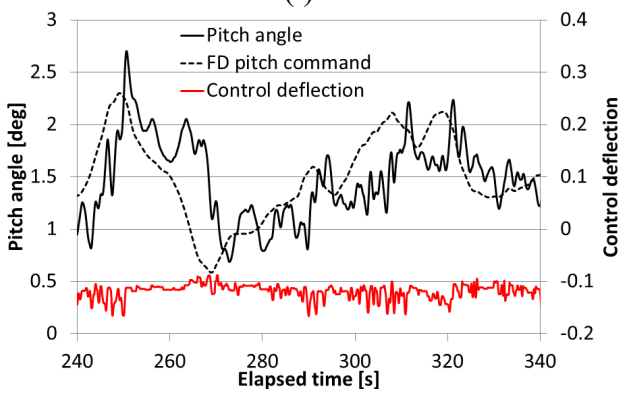

Fig. 4 Longitudinal control and movement of data (i)-1.

2.4 Differences between Pitch Control and Roll Control

Four control characteristics are identified in pitch control as described in Sec. 2.5, and it is investigated whether each characteristic is also observed in roll control.

1) Stochastic behavior

Roll control is obviously stochastic, because a human pilot cannot duplicate hiso control even when given the same condition. The overshoot of control is also observed in roll control around 320 s.

2) Periodic behavior

The periodic control is also observed in the roll control.

3) Discrete behavior

The discrete control is also observed in the roll control.

4) Half control

The half control is observed in pitch movement around 270. When the pilot uses half control, the pitch angle decreases once and increases a little due to periodical control (braking control). Next, the pitch angle decreases again. The same characteristic is observed in roll control around 265 s, 310 s, 325 s, for example. On the other hand, a large tracking delay is observed in pitch control, while little delay is observed in roll control. This might be due to the fast convergence of roll dynamics. The control strategy itself might also vary between pitch and roll controls.

Based on these results, the author has concluded that the roll control and pitch control characteristics are the same in principle, with a difference in the control magnitude. The biggest difference is found in the command tracking delay. The roll angle seems to follow the FD roll command with a small delay. It is assumed that the pilot control strategy itself is the same between roll and pitch control. Therefore, the same pilot control model can be applied.

3. Pilot Control Model and Its Verification

3.1 Proposed pilot model

This subsection provides a summary of the proposed pilot model. Since the concept of the

model is already proposed in the previous research[2], this paper presents the flow of the pilot model calculation only.

First, the proposed pilot model flow is shown in Fig. 5. To model the periodic control, the main control part is split into two parts called “P control” and “D control”. P control denotes proportional control, when the pilot moves the control stick to follow the FD command. “D control” denotes derivative control, when the pilot moves the control stick opposite to the “P control” to brake the pitch/roll movement. A single control loop consists of both P control and D control. At the beginning of the control loop, the pilot perceives the current status, and he decides on several action parameters such as the target roll angle.

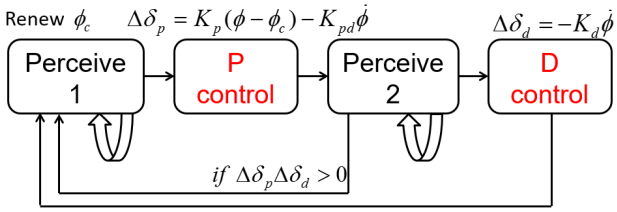

Fig. 5 Proposed pilot model flow.

In the “perceive” state, the pilot decides whether to move the control stick or not. If the required roll adjustment is little, the pilot tends not to move the control stick. The target roll angle is not necessarily the same as the FD roll command to express half control. The target roll angle for the pilot (ϕ_c) is calculated by the following expression.

$$\phi_c = \phi + \alpha(\phi_{FD} - \phi) \qquad (1)$$

where ϕ is the observed roll angle, ϕ_{FD} is the observed FD roll command, and α is the half control parameter. Since the human pilot recognizes the situation with delay, an “observed” value at 0.2 s before the current time is used. To model the half control precisely, α should be 0.5. However, the pilot does not operate the exact half control, so g is assumed to follow the gamma distribution with a scale parameter a and a shape parameter b. α is calculated by the following expression.

$$\alpha = \alpha_{center} - g \qquad (2)$$

where α_{center} is a parameter. The required control adjustment is calculated by the following expression.

$$\Delta\delta_p = K_p(\phi-\phi_c)-K_{pd}\dot{\phi} \qquad (3)$$

where K_p and K_{pd} are parameters. Based on $\Delta\delta_p$, the pilot chooses whether he should move the control stick or not. The probability that he moves the control stick is calculated by the following expression.

$$p(\Delta\delta_p) = \frac{1-p_0}{1+\exp(-\sigma(|\Delta\delta_p|-\tau))} \qquad (4)$$

where p_0, σ, τ are the parameters. $p(\Delta\delta_p)$ is a monotonically increasing function with $\Delta\delta_p$, so the pilot is more likely to act when the required control is large. Once he does not move the control stick, he stays at a perceive state, and perceives the current status again after t_{int1}. t_{int1} follows a normal distribution with average $t_{\text{int1\_ave}}$ and standard deviation $t_{\text{int1\_sig}}$ .Otherwise, the pilot moves the column. The new column position is calculated by the following equation.

$$\delta + \Delta\delta_p + e \qquad (5)$$

where δ is the current column position, and e indicates the control noise with average 0 and standard deviation Σ . In reality, the pilot control is not a complete discrete control, and it moves based on the calculated column movement time. This will be explained later.

After P control, the pilot moves to perceive 2 state. At perceive 2 state, the required control adjustment is calculated by the following expression.

$$\Delta\delta_d = -K_d\dot{\phi} \qquad (6)$$

where K_d is the parameter. If $\Delta\delta_p\Delta\delta_d > 0$, the control direction of both P control and D control is the same, which does not result in braking in D control. In such a case, D control is skipped and the pilot goes back to perceive 1 state. Otherwise, the pilot moves the control stick with a probability of p_0 . Otherwise, the pilot stays at perceive 2 state, and perceives the

current status again after $t_{\text{int}2}$. $t_{\text{int}2}$ follows a normal distribution with average $t_{\text{int}2\_ave}$ and standard deviation $t_{\text{int}2\_sig}$. If the pilot moves the control stick, the new control position is calculated by Eq. (5), then he goes back to perceive 1 state. By introducing both P control and D control, the periodical movement can be modeled. The stochastic tracking capability can be achieved by adjusting α .

As for the discrete movement, the pilot control is not completely discrete. Fig. 6 shows the relationship between the control amount and the control time. Based on this figure, the control time $\Delta t_{control}$ is expressed by the following expression.

$$\Delta t_{control} = x\left(\Delta\delta\right)^{y} \tag{7}$$

where x and y are the parameters. According to Fig. 6, the actual column movement time seems to include noise around the regression line. Therefore, the column movement time is set as the average of $x\left(\Delta\delta\right)^{y}$ and standard deviation of $x\left(\Delta\delta\right)^{y}\sigma_{xy}$. Also, once the pilot moves the control stick, minimum control amount seems to exist, which is defined as $\Delta\delta_{\min}$.

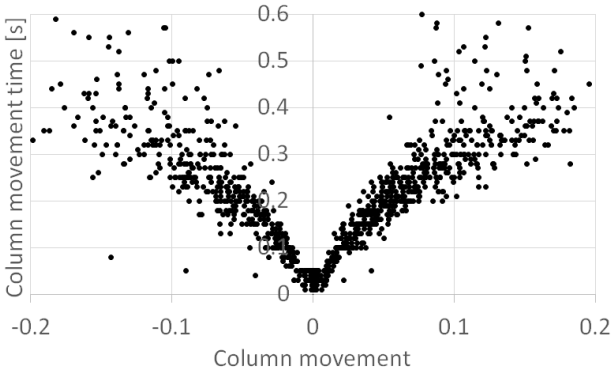

Fig. 6 Relationship between column movement and column movement time.

3.2 Parameters Estimation

To develop a pilot model, a total of 18 parameters are required. The required parameters are summarized in Table 2. x and y are obtained directly from data, so the remaining 16 parameters should be estimated.

Table 2 Summary of parameters.

Parameters	Explanations
σ, τ	Parameter of state transition probability at perceive 1 state
p_0	Probability of failure of state transition
K_p, K_{pd}	Gains in P control state
K_d	Gains in D control state
$t_{\text{int}1\_ave}, t_{\text{int}1\_sig}$, $t_{\text{int}2\_ave}, t_{\text{int}2\_sig}$	Parameters of time interval of perceiving states
Σ	Standard deviation of control noise e
α_{center}, a, b	Half control parameters
x, y, σ_{xy}	Column movement time parameters
$\Delta\delta_{\min}$	Minimum column movement

The parameter estimation is done using the actual pilot control data to mimic the pilot control characteristics. Therefore, the parameters are optimized to minimize the following objective function g.

$$\begin{aligned} g = \sum_i \log\left(\frac{\omega_{i+1}}{\omega_i}\right) \\ \left\{ w_1 \left(\log(f_{act}^{column}(\omega_i)) - \log(f_{\text{model}}^{column}(\omega_i))\right)^2 \right. \\ + w_2 \left(\log(f_{act}^{FD}(\omega_i)) - \log(f_{\text{model}}^{FD}(\omega_i))\right)^2 \\ \left. + w_3 \left(FD_{act} - FD_{\text{model}}\right)^2 \right\} \end{aligned} \tag{7}$$

where w_1, w_2, w_3 are the weight parameters and $f(\omega)$ indicates the amplitude at frequency ω . FD indicates the root mean square error (RMSE) of FD command. As for the first two terms, the column movement and FD command of both actual data and simulation data are converted to the amplitude at each frequency using Fourier transform. The difference of amplitude at each frequency should be minimized. As for the third term, RMSE of FD shows the average FD tracking capability through a single landing. By trial and error, three weight parameters are set as follows: $w_1 = 3, w_2 = 2, w_3 = 5$. Since the proposed model has a stochastic component, 50 landing simulations are conducted and both the average

and the best case result are included in the objective function. Its weight parameter between the average and the best case is defined as β, and set to 0.5. The final objective function is described in the following equation.

$$\beta g_{best} + (1-\beta) g_{average} \quad (8)$$

The parameters are optimized via Real-Coded Genetic Algorithm (RCGA). The parameters are summarized in Table 3.

Table 3 Parameters of RCGA.

Parameters	Values
Populations	100
Number of generations	300
Selections	MGG[4]
Crossover	Simplex[5]
Number of crossover	96

Each simulation starts at an altitude of 1850 ft. The other initial conditions (e.g. pitch angle, horizontal position) are set the same as in the actual data. The objective function is calculated with the data correspondent to an altitude between 1800 ft and 500 ft. A single pilot model is made with a single landing data, and a total of 5 pilot models are constructed. The pitch and throttle controls are given by the autopilot and autothrottle, and only the roll control (aileron control) is exerted by the proposed model.

4 Simulation Results

4.1 Qualitative simulation analysis

Using a proposed pilot model with the optimized parameters, a landing simulation can be conducted. First, the time histories of the roll angle, FD command, and control deflection are shown in Fig. 7. Since the proposed model is stochastic, different simulation result is obtained in each landing simulation. Fig. 7 shows an example of a single landing simulation. It is seen that the pilot control characteristics, such as half control, periodical and discrete movement, are modeled well. The observed roll angle range is between –1.5 and 1.0 deg, which is similar to the data in actual flight as shown in Fig. 3. In addition, a roll oscillation with about 1 deg magnitude and about 20 s time period is observed throughout a simulation, but a short term oscillation with small magnitude is also observed around 60-90 s. This phenomenon is also observed in the obtained flight data. This means that a single pilot model with stochastic components is sufficient to model various pilot control characteristics.

For comparison purposes, Fig. 8 shows the time history of the simulation with autopilot. The time histories of roll angle are different from those in obtained flight data and pilot model simulation. No periodical movement is observed, and the FD command tracking capability is also much better. The proposed model can capture the pilot control characteristics, which are difficult to obtain based on the conventional control strategy.

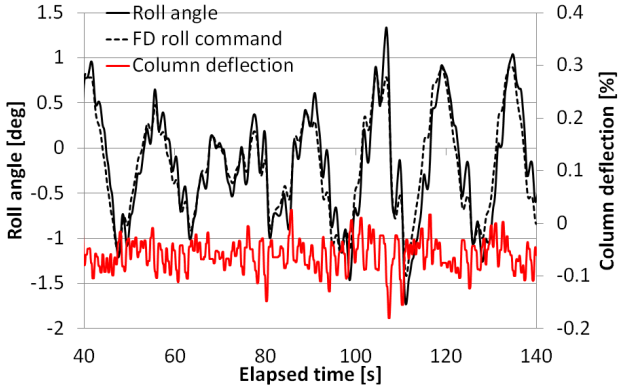

Fig. 7 Lateral control and movement data with pilot model (i)-1.

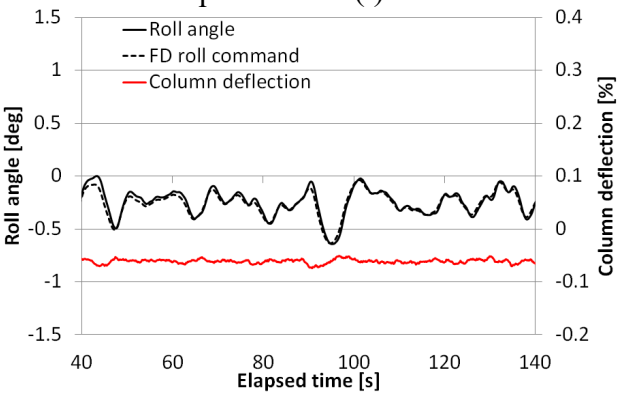

Fig. 8 Lateral control and movement data with autopilot.

4.2 Lateral displacement and FD command tracking capability

Next, lateral displacement is considered. As described before, the purpose of this

research is to calculate the probability contour of the deviation from the nominal path, so the deviation characteristics are the most important. Since the proposed model is stochastic, 100 landing simulations are conducted in each pilot model and wind condition, and lateral deviation characteristics are observed. The lateral displacement is evaluated by the RMSE of lateral deviation. Fig. 9 shows the RMSE of lateral deviation for actual data, 95 % range by pilot model simulations, and autopilot. Fig. 10 shows the RMSE of FD tracking for actual data and 95 % range by pilot model simulations. As expected, both RMSE of lateral deviation and RMSE of FD for actual data are the largest under strong wind ((ii)-1). On the other hand, under no wind, neither RMSE of lateral deviation nor RMSE of FD are the smallest. Using autopilot, the smallest RMSE of lateral deviation is observed under strong wind ((ii)-1). Although the wind used in the simulation is not strong, no clear relationship between the RMSE of lateral deviation and wind condition has been observed. However, the actual data of both RMSE of lateral deviation and RMSE of FD fall into the 95 % range of pilot model simulations, which means that the proposed pilot model can simulate the deviation characteristics. Since the RMSE of lateral deviation is not included in the objective function, the agreement of RMSE of lateral deviation also supports the validity of the proposed model. One might say that RMSE of lateral deviation is closely related to RMSE of FD which is included in the objective function. Fig. 11 shows the relationship between RMSE of lateral deviation and RMSE of FD for 100 simulations under pilot model (i)-1. Although there is a relationship between these two factors, its correlation is not so strong. The FD tracking capability is not necessarily closely related to the deviation characteristics.

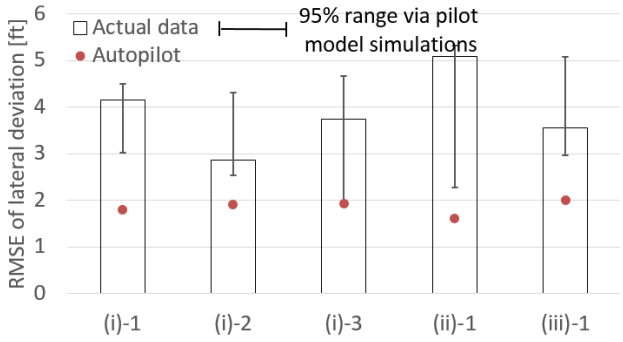

Fig. 9 RMSE of lateral deviation for actual data, 95 % range by pilot model simulations, and autopilot.

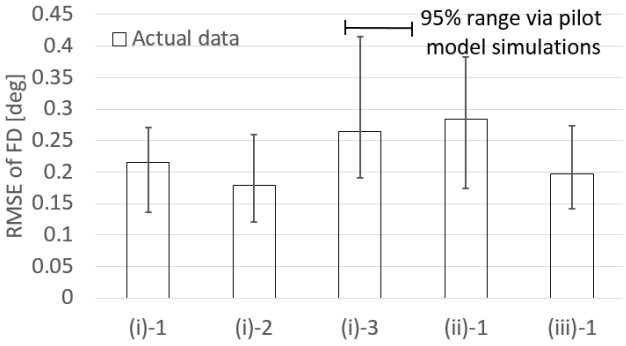

Fig. 10 RMSE of FD tracking for actual data and 95 % range by pilot model simulations.

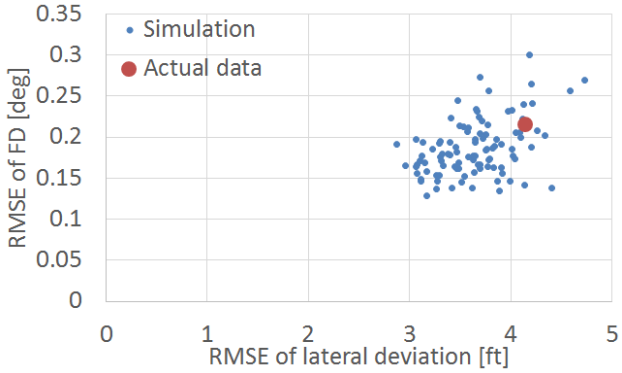

Fig. 11 Relationship between RMSE of lateral deviation and RMSE of FD.

6 Conclusions

In this paper, a new pilot control model was proposed. We focused on two pilot control characteristics: stochastic and periodical movement. Since the previous work modeled the longitudinal control, this paper focused on lateral control. The lateral control also had similar characteristics like longitudinal control, and the same modeling method was applied. The simulation results showed that the proposed model seemed to capture the pilot control

characteristics. In the future, more pilot control data will be obtained, and differences of pilot control strategy will be investigated.

References

[1] "Procedures for Air Navigation Service — Aircraft Operations (PANS-OPS)," International Civil Aviation Organization, Doc 8168, Montreal.
[2] Mori, R., "Development of Pilot Model with Stochastic Periodical Discrete Movement," *Proceedings of IEEE International Conference of Systems, Man, and Cybernetics*, pp. 1532-1538, 2015.
[3] Federal Aviation Administration, "Criteria for Approval of Category III Weather Minima for Takeoff, Landing, and Rollout," AC 120-28D, 1999.
[4] H. Satoh, M. Yamamura, and S. Kobayashi, "Minimal generation gap model for GAs considering both exploration and exploitation," Proc. 4th Int. Conf. Soft Comput., 1996, pp. 494–497.
[5] S. Tsutsui, M. Yamamura, and T. Higuchi, "Multi-parent recombination with simplex crossover in real coded genetic algorithms," Proc. Genetic Evol. Comput. Conf., 1999, pp. 657–664.

6 Contact Author Email Address

r-mori@mpat.go.jp

Copyright Statement